Applications of High Throughput (Combinatorial) Methodologies to Electronic, Magnetic, Structural, and Energy-Related Materials ☆

Howie Joress and Martin L Green, National Institute of Standards and Technology, Gaithersburg, MD, United States
Ichiro Takeuchi, University of Maryland, College Park, MD, United States
Jason R Hattrick-Simpers, National Institute of Standards and Technology, Gaithersburg, MD, United States

Introduction and Historical Perspective

High-throughput materials science, formerly referred to as combinatorial materials science, is a paradigm for materials discovery and optimization that relies on rapid, often parallelized, synthesis and characterization. These methodologies grew out of the pharmaceutical industry and rapidly spread to other fields, several of which have matured and been the subject of review articles: organic coatings (Chisholm and Webster, 2007), sensor materials (Potyrailo and Mirsky, 2008), inorganic materials (Koinuma and Takeuchi, 2004), catalysis (Dellamorte et al., 2009; Kirsten and Maier, 2004; Maier et al., 2007), and functional materials (Xiang et al., 1995; Takeuchi et al., 2002).

High-throughput experimentation (HTE) (Barber and Blamire, 2008; Maier et al., 2007; Green et al., 2013) typically involves creation of a "library" of samples that contains a variation in one or more parameters, most commonly this variation is in composition, but it can also be variation in processing parameters such as annealing temperature. Each sample in the library is then rapidly and locally measured using automated methods to probe for variation in the properties of interest as a function of composition/processing, resulting in the generation of a large data set. Recently, these methods have been modified to allow for on-demand synthesis in a closed loop with characterization to allow for autonomous machine learning driven studies (Shimizu et al., 2020; Boyce and Uchic, 2019). In the study of inorganic materials, the vast majority of these libraries are created in a thin-film form factor. The idea of utilizing deliberately created composition gradients in co-deposited thin films to obtain significant portions of phase diagrams in a continuous composition spread can be traced back to about fifty years ago for various ternary systems (Boettcher et al., 1955).

Combinatorial methodologies are generally faster and less expensive (likely true even taking initial equipment investments into account) than traditional (e.g., "one composition at a time") approaches (Maier et al., 2007). Further, since all experiments are carried out on the same library sample with the same measurement tool over a short time period, most systematic errors are eliminated, thus generating a comprehensive and reliable data set. Combinatorial materials science excels in the observation of trends and in screening, i.e., finding the "sweet spot" of the response surface, which enables rapid materials optimization.

In spite of the large number of papers published in the field of combinatorial materials science, industry has not adopted the new paradigm on a large scale, and there has been some skepticism. Some of this is due to the nature of the library films, which may contain local variations such as microstructural changes and stress variations that result directly from compositional variations; thus, the libraries are perceived as flawed, in that although only one variable is intentionally varied, other properties may change unintentionally, resulting in a perceived "unscientific" approach. While it is difficult to fully defend the notion that the composition of a library film can be varied while maintaining all other properties constant, the use of a greater number of analysis techniques should allow these complicated interactions to be sorted out (Barber and Blamire, 2008).

☆Portions of this work are adopted from Green et al.

Another source of criticism is the frequent necessity to process the combinatorial library samples using different growth and post-growth processing techniques than will be employed in the production of the material for its intended application. This criticism can be mitigated to some extent by realizing that in combinatorial analysis, the variation of the property, particularly maxima and minima, with regard to the underlying processing/compositional variation can be more important than the absolute value of the property at any given value of the parameter. Even so, to resolve this issue in combinatorial experiments, the results should be benchmarked to some key data that have been determined by more traditional means and optimal results should be reproduced as well. Combinatorial materials science has traditionally been focused on materials discovery, screening and optimization, to combat the extremely high cost and long development time of new materials and their introduction into commerce. Going forward, this new paradigm may be driven by other needs such as materials substitution, and experimental verification of materials properties predicted by modeling and simulation.

Here we discuss HTE methodologies applied to a range of topic areas including silicon microelectronics, magnetic materials, phase change materials, energy material, structural materials, and shape memory alloys. We try to describe both relevant methodologies as well as interesting results in each area, showing examples that can be benchmarked against traditional measurements. Further, we aim to point to useful reviews where additional information on a given topic can be found.

Silicon Microelectronics and Advanced Metal Gate Materials

Continuous scaling of complementary–metal–oxide–semiconductor (CMOS) transistors to meet the evolving requirements of the International Technology Roadmap for Semiconductors (ITRS) has made the traditional gate stack, SiO_2 gate dielectric and poly-crystalline Si (poly-Si) gate electrode, unsuitable for future integrated circuit devices. Further, only about a dozen elements were involved in integrated circuit manufacturing in 1990, as opposed to over fifty by the year 2000. The introduction of so many new elements and materials in the form of both alloys and compounds was an excellent opportunity for the widespread use of combinatorial methodologies in the microelectronics industry. Development of high-κ dielectrics has been a large effort in the combinatorial space, and, beyond the scope of this work, is reviewed in Green et al. (2013). Here we focus on combinatorial work on the development of novel metal-gate electrode materials. Substitutes for the poly-Si gate electrodes using true metals or metalloids can provide higher carrier densities and therefore lower resistivities as well as less carrier depletion. For high performance CMOS applications, the metal gate electrodes must have work functions (Φ_m) that are aligned with the conduction (4.05 eV) and valence (5.17 eV) bands of Si for n-channel metal–oxide–semiconductor (NMOS) and p-channel metal–oxide–semiconductor (PMOS) applications, respectively.

In one of the first high throughput studies of metal gate electrodes, Ni–Ti–Pt ternary libraries were deposited by magnetron sputtering through moving masks on HfO_2 dielectrics as shown in **Fig. 1**, and studied systematically by WDS, micro-XRD, capacitance-voltage (C-V), and current-voltage (I-V) analyses (Chang et al., 2006). A more negative flatband voltage (V_{fb}) was observed close to the Ti-rich corner than to the Ni- and Pt-rich corners, implying a smaller Φ_m near the Ti-rich corner, and higher Φ_m near the Ni- and Pt-rich corners. Not only is that observed but also the Φ_m values measured for the nearly pure metals (i.e., near the corners) in this combinatorial experiment are in very good agreement with bulk literature values for Ni, Ti, and Pt. Thus, combinatorial methodologies proved to be accurate and useful in surveying the large compositional space of ternary alloy metal gate electrode systems.

Metalloids such as metal nitrides and carbides have attracted attention as potential gate metal electrodes due to their superior thermal and chemical resistance compared to metals. Among the many metal gate candidates, TaN has shown very useful Φ_m tunability through alloying with various elements (Alshareef et al., 2006; Park et al., 2003). In particular, $Ta_{1-x}Al_xN_y$ alloys are easily deposited, with very good electrical and chemical properties (Park et al., 2003). The $Ta_{1-x}Al_xN_y$ system is an ideal combinatorial materials science problem because systematic measurement of Φ_m across the wide composition range, x, is not trivial, since capacitor fabrication and characterization based on a "one-composition-at-a-time" approach are extremely time consuming; thus very little data is available for this metal gate alloy system (Alshareef et al., 2006). Recently, a combinatorial approach was applied to Φ_m extraction for the metal gate electrode system $Ta_{1-x}Al_xN_y$ deposited on HfO_2 (Chang et al., 2008). Over two thousand capacitors on four identical metal gate libraries (albeit with differing capacitance due to SiO_2 underlayers of different thicknesses), were automatically measured, from which V_{fb} shifts were extracted, and Φ_m determined. **Fig. 2** shows the array of test capacitors in the library sample; although a composition range of $0.05 \leq x \leq 0.85$ was achieved on the library, electrical measurements were only performed on samples with $0.05 \leq x \leq 0.50$, because higher Al concentrations were not suitably conductive. As can be seen from **Fig. 3**, Φ_m of the $Ta_{1-x}Al_xN_y/HfO_2/SiO_2/Si$ gate stack structures can be tuned as a function of gate metal composition over a wide composition range, as well as by annealing. From these results, it was suggested that $Ta_{0.9}Al_{0.1}N_{1.24}$ gate metal electrodes may be useful for PMOS applications. **Fig. 3** is a noteworthy example of the power of the combinatorial technique. In this graph, Φ_m is shown as a function of gate metal composition, with about thirty compositions represented, as opposed to isolated data for only a few of those composition points found in the literature. Further, the data instantly reveals two other phenomena. First, one can see the consistent increase in Φ_m after anneals at higher temperatures than the initial forming gas anneal (500°C), and second, one observes the range of the thermal instability after the 1000°C anneal, for gate electrodes containing less than about 27% Al. Consistent and comprehensive sets of working data such in **Fig. 3** are almost non-existent in the semiconductor microelectronics literature.

Magnetic Materials

Magnetic phenomena have historically played profound roles in the advancement of human civilization; the technological foundation of modern society is built upon the development of magnetic materials. Today, magnetic materials and devices

(a)

(b)
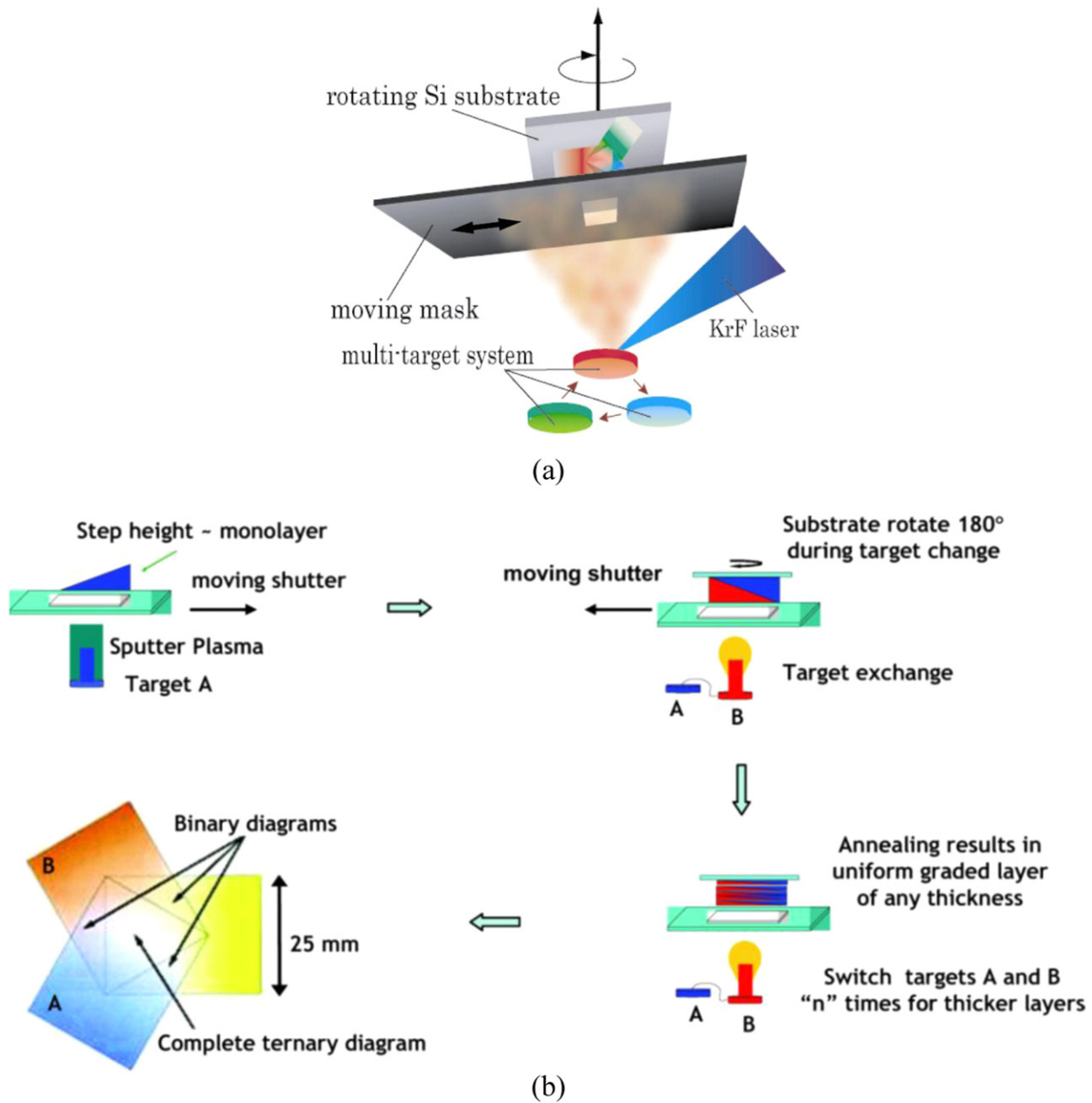
Fig. 1 (a) Schematic illustration of the ternary and binary composition spread method with sample rotation and moving mask system, first employed by Fukumura et al., 2000. Here, the PLD deposition method is shown as an example, but ion beam sputtering can also be used. (From T. Chikyow et al., 2006). (b) SCHEMATIC showing the synthesis of a combinatorial "library" of the binary system A-B. A thin wedge (wedge height 0.5 nm) of A is deposited, and the substrate is rotated 180. A complementary wedge of B is then deposited. This is repeated "N" times, until the desired film thickness is achieved. If the substrate is rotated 120 instead, a ternary (shown from above in the lower left), rather than a binary alloy system may be synthesized (from M.L. Green et al., 2013).

are ubiquitous in everyday life. For example, the steady rate at which the maximum energy product, $(BH)_{max}$, of permanent magnets has increased over the past decades led directly to continuous improvements in electric motor technology. Further, magnetic memory, a key technology for information technology, recording and sensing devices is at the heart of a massive industry.

Demand for higher performance magnetic materials in a wide range of technologies continues, and these applications represent ideal platforms for implementing combinatorial strategies. At the same time, fundamental scientific investigations into novel magnetic phenomena continue to uncover exotic effects such as multiferroicity and topological dielectricity. Exploration of such effects and their underlying physical mechanisms is directly tied to mapping of their phase diagrams. To this end, CCS experiments have been exploited to discover new compositions with improved properties, as well as to understand composition-structure-property relationships.
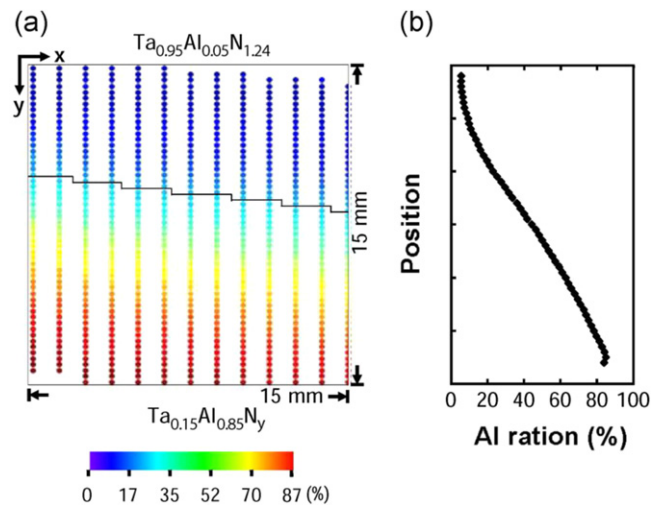
Fig. 2   (a) Composition map of the Ta1−xAlxNy composition spread, as determined by WDS. The dimension of the library is 15 mm × 15 mm. Each dot represents a capacitor, and (b) plot of the composition variation across the sample. A wide composition range, x = 0.05–0.85, was achieved (from Chang *et al.,* 2008).
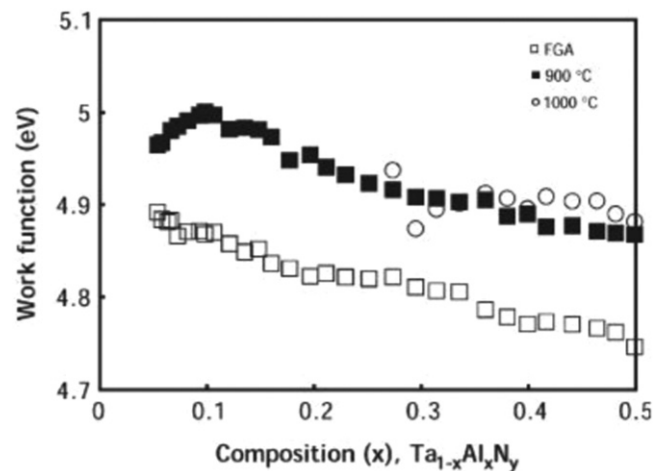
Fig. 3   Plot of the extracted work functions (Φm) for the Ta1−xAlxNy composition spreads. Φm was extracted as a function of Al content after a forming gas anneal (500°C), and 900°C and 1000°C rapid thermal anneals. After the 1000°C anneal, for x < 0.27, Φm could not be mapped due to degradation of the capacitors (from Chang *et al.,* 2008).

High Throughput Magnetic Characterization Techniques

A number of non-destructive scanning probe techniques have been used to map magnetic properties from combinatorial libraries (Fukumura *et al.,* 2000; Yoo and Tsui, 2002; Yoo *et al.,* 2001; Famodu *et al.,* 2004; Takeuchi *et al.,* 2003). As is the case for combinatorial measurements in general, a significant challenges lies in extracting accurate quantitative values of magnetic properties from a particular location on a library film, such that the value is in agreement with that obtained from a discrete sample of the same composition, using a standard "bulk" measurement technique such as a superconducting quantum interference device (SQUID) magnetometer. Significant actual variation in some physical properties between bulk and thin film materials of the same composition are often the cause of the lack of agreement.

While there exist many important magnetic properties to be characterized, the net (i.e., remnant) magnetization is by far the most important property for screening of novel magnetic materials. Various techniques can be used to obtain magnetic field distributions emanating from thin film combinatorial samples to characterize this property. They include scanning SQUID microscopy (Famodu *et al.,* 2004; Fukumura *et al.,* 2000; Takeuchi *et al.,* 2003) and the scanning Hall probe technique (Yoo *et al.,* 2001). Although the magnetic field distribution itself does not yield the value of the magnetization, in principle one can extract it using calibration samples. In the absence of an external applied field, remnant magnetization may be measured (Yu *et al.,* 2005).

The magnetic-optical Kerr effect (MOKE) technique (Yoo and Tsui, 2002; Yoo et al., 2001) is based on the fact that the polarization of light is rotated upon reflection from the surface of a magnetic material, and further that the rotation angle is directly proportional to the magnetization. MOKE is particularly useful since one can map the magnetic hysteresis loop from different positions on combinatorial samples by sweeping the applied magnetic field, from which one can obtain the saturation magnetization (through calibration) as well as the coercive field values.

The scanning Hall probe can also be used to map saturation magnetization values (Yoo et al., 2001). In order to obtain absolute values of magnetization from the measured magnetic field without calibration, an inversion technique has been developed which can be applied to any spatially resolved field distribution data (Aronova, 2004). This technique uses a computational algorithm which performs an inverse Fourier transform to calculate magnetic pole densities, which in turn is integrated to obtain magnetization values at any location on the library. This algorithm has been applied to analysis of RT scanning SQUID microscopy data from a variety of magnetic material libraries (Famodu et al., 2004; Matsumoto et al., 2003; Takeuchi et al., 2003). In particular, it has been applied to thin film composition spreads of ternary metallic alloy systems containing ferromagnetic shape memory alloy (SMA) phases. Critically, the remnant magnetization values determined for the CCS library were demonstrated to be in good agreement with values measured by SQUID and vibrating sample magnetometers for single composition, large scale thin films (Takeuchi et al., 2003).

Magnetic Metallic Alloys and Magnetic Phase Diagrams

The search for novel magnetic materials led to some of the original high throughput experiments and techniques (Hanak and Gittleman, 1972). Magnetic alloys were screened for several different functional properties, targeting specific applications including recording heads and inductor cores, using co-sputtering techniques to create thin film libraries suitable for rapid phase mapping.

To date, less than 5 % of all possible ternary metal phase diagrams have been investigated; even fewer systems exist for which magnetic properties have been mapped. Phase diagrams mapped using thin CCS film libraries must be regarded as "thin film phase diagrams." Composition-structure-property relationships deduced from thin film libraries can differ from those obtained using bulk samples. Fortunately, however, most high technology devices comprise highly integrated multilayer thin film structures, and thin film phase diagrams are often more relevant than bulk phase diagrams in understanding and modeling these devices. While mapping of magnetic properties alone can provide great insight, correlating these properties with phase structure across composition is much more valuable. Such correlations have only been recently carried out; the key facilitating factors for such an integrated approach are the advent of computer technology and the use of sophisticated measurement instrumentation. A good example of comprehensive mapping of the structural and magnetic properties of a phase diagram using the CCS spread method is the experiment of Yoo et al. (2006). The Fe-Ni-Co system was deposited onto a triangular sapphire substrate by sequential ion beam deposition of the elemental metals at RT, followed by extensive annealing in vacuum (600°C at 10^{-6} Pa) to allow complete interdiffusion of the layers and crystallization. XRD was used to obtain the structural phase distribution. A 4° 2θ range (42 to 46°) contained all of the major diffraction features in the phase distribution. For a given structural phase, the X-ray peak intensity allows one to track the compositional range. Regions in which phases coexist could be identified by looking for diffraction peaks arising from multiple phases. It was observed that near the phase boundaries, the full width half maximum of the peaks tended to increase. **Fig. 4(a)** shows the distribution of phases deduced from the library sample; fcc Ni, bcc Fe and fcc and bcc Ni-Fe alloys are present. This result is consistent with the known bulk structural phases in this alloy system. The magnetic properties of the library film were investigated by MOKE, **Fig. 4(b)**. A qualitative saturation magnetic moment of each point of the ternary phase diagram was mapped at applied magnetic fields of $+/- 50$ Oe (3979 A/m). Comparison of the two figures shows a clear correlation between the phase distribution and the magnetization; the bcc Fe has the highest magnetization. Further, the observed magnetization variation is consistent with the known concentration-dependent saturation induction of the Fe-Ni-Co system deduced using the traditional bulk method, **Fig. 4(c)** (Bozorth, 1993). Although MOKE analysis does not allow direct quantitative measurement of magnetization, by comparing the measured Kerr rotation angle with values obtained on calibration samples using standard methods such as SQUID magnetometry, one can convert the Kerr angle map to a magnetization map. In this particular ternary experiment, a mechanical hardness map was also obtained using nanoindentation, which revealed that the Fe-Co region, consisting of fcc and bcc (two phase) or pure bcc (single phase) areas, is harder than the higher Ni concentration fcc region.

Phase Change Materials

Phase-change materials (PCM), most often semiconducting or semi-metallic alloys (also known as chalcogenide compounds) containing S, Se, or Te, have both optical and electrical storage applications. Upon heating, PCM's undergo a reversible phase transformation from a supercooled, metastable amorphous phase to a crystalline phase. The amorphous phase has significantly lower reflectivity than the crystalline phase, making them the material of choice for rewriteable optical storage media (e.g., compact disks). PCM's also have a low electrical resistance in the crystalline phase, which may increase by many orders of magnitude in the amorphous phase, making them very useful for storage applications as non-volatile flash memories in integrated circuits (Ielmini and Lacaita, 2011).

To achieve high write and erase rates for memory storage, the kinetics of the phase transformation between the amorphous and crystalline phases must be very fast in both directions. The Ge–Sb–Te ternary alloys are used for optical storage applications (Yamada, 1996). Alloys for nonvolatile memory applications also require fast kinetics, but other factors such as low power consumption and cycling endurance are also important. Despite the interest in the Ge-Sb-Te system, there have been few combinatorial experimental

(a)

(b)

$$\theta_K^{abs} \propto (M_s^+ - M_s^-)/2$$

$$M_s \propto \theta_K^{abs}$$

(c)
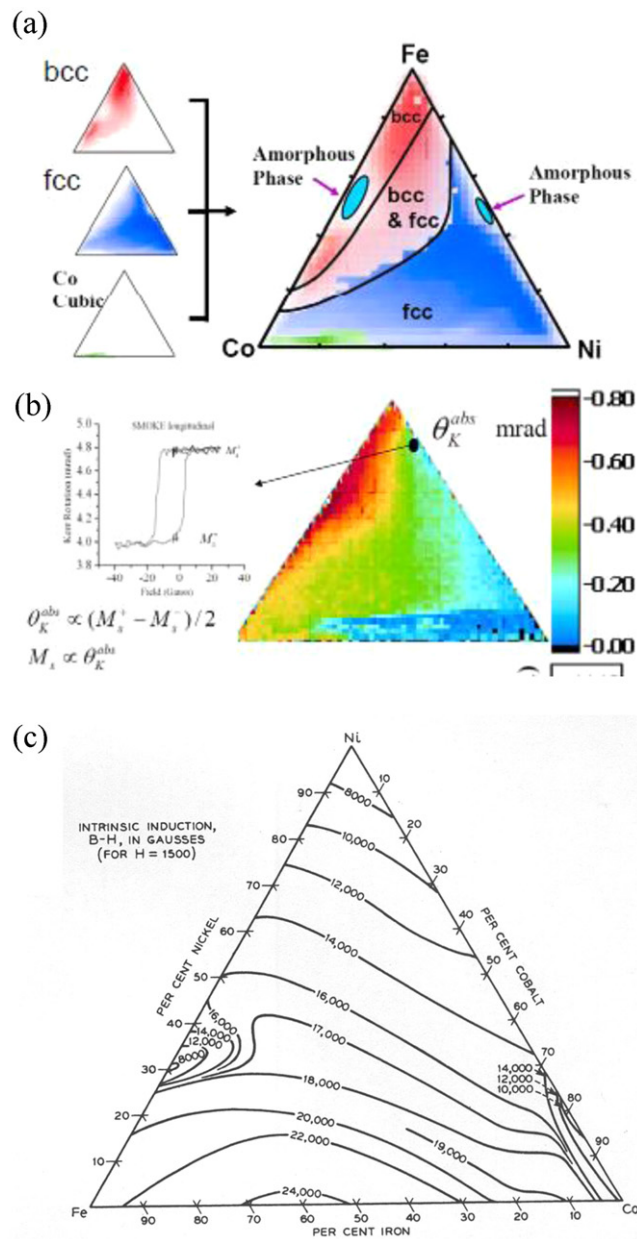
Fig. 5–80.   Saturation induction (approximate) of annealed Fe-Co-Ni alloys.

Fig. 4   Mapping of properties of a Fe-Ni-Co combinatorial thin film library, from Yoo et al.114; (a) The Fe-Ni-Co phase diagram obtained from distribution of structural phases deduced from X-ray microdiffraction peaks of fcc, bcc and "Co cubic" phases, and (b) mapping of magnetic property using scanning magneto-optical Kerr effect measurement. The Kerr rotation angle measured at $+/-$ 50 Oe applied field is plotted. The figure at left shows a typical hysteresis loop, and (c) saturation induction mapped for the Fe-Ni-Co ternary phase diagram using the traditional individual alloys for comparison, (from Bozorth, R.M., 1993. Ferromagnetism. New Jersey: Wiley-IEEE Press).

studies. Kyrsta *et al.* (2001) used CCS Ge–Sb–Te films to investigate crystallization and writing times. They showed that ternary compositions at or near the GeTe–Sb$_2$Te$_3$ pseudobinary tie line exhibit fast (70 nsec to 150 nsec) crystallization behavior.

Energy-Related Materials

Thermoelectrics

Thermoelectric materials, which enable the direct solid state conversion of thermal to electrical energy, have important applications for utilization of waste heat energy (particularly vehicular engine heat) via the Seebeck effect, as well as solid state refrigeration via the

Peltier effect (Kanatzidis et al., 2003). However, at present the best thermoelectric conversion materials and devices are not efficient enough for widespread commercial use. The availability of higher conversion efficiency thermoelectric materials will play a significant role in their implementation. High conversion efficiency thermoelectric devices require materials that possess large figures of merit, ZT, which is equal to $S^2\sigma T/\kappa$, where S is the Seebeck coefficient, σ the electrical conductivity, κ the thermal conductivity, and T the absolute temperature. Combinatorial approaches have been used to optimize and discover thermoelectric materials through measurement of S, σ, and therefore $S^2\sigma$ (another thermoelectric figure of merit, known as the power factor) (Wong-Ng et al., 2014). One such tool for performing power factor screening is illustrated in **Fig. 5**. To obtain ZT, the thermal conductivity of the film must also be measured. This is a notoriously difficult measurement to perform, especially on a combinatorial thin film library, because of the need to measure the film while thermally clamped to the substrate which generally has much greater thermal transfer; however, high throughput measurements of thermal conductivity have also been performed, as will be discussed below.

An example of a class of thermoelectric materials that was studied is the $Mg_xSi_yGe_{1-y}$ ternary system, where x was varied between 2.3 and 4.5, and y between 0.45 and 1, on a discrete PLD film library sample (Watanabe et al., 2008). The library was deposited onto an alumina substrate with prefabricated localized heaters and contact leads. Temperature gradients across the sample, as well as the base temperature of the samples (which varied between RT and 673K), were measured with an IR camera. The measurements were first calibrated using a constantan film, whose Seebeck coefficient and resistivity were found to be very close to the bulk values. Seebeck coefficient and resistivity results for this ternary library film are depicted in **Fig. 6**.

Thermoelectric metal alloys have been studied using high throughput methods (Yamamoto et al., 2007). $Ni_{1-x}Cu_x$ library samples, where x spanned the entire range from 0 to 1, were prepared in two different ways. The first set was prepared by powder
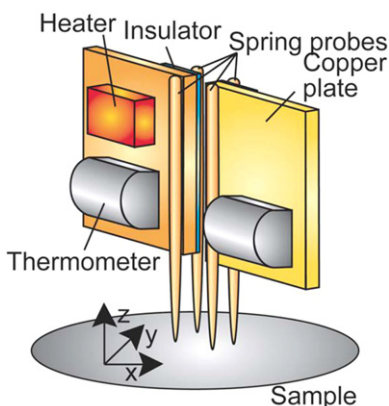
Fig. 5 Schematic diagram of measurement probe to measure electrical conductivity and Seebeck coefficient (from Otani, M., Lowhorn, N.D., Schenck, P., et al., 2007. A high-throughput thermoelectric power-factor screening tool for rapid construction of thermoelectric property diagrams. Applied Physics Letters 91 (13), 132102. doi:10.1063/1.2789289).
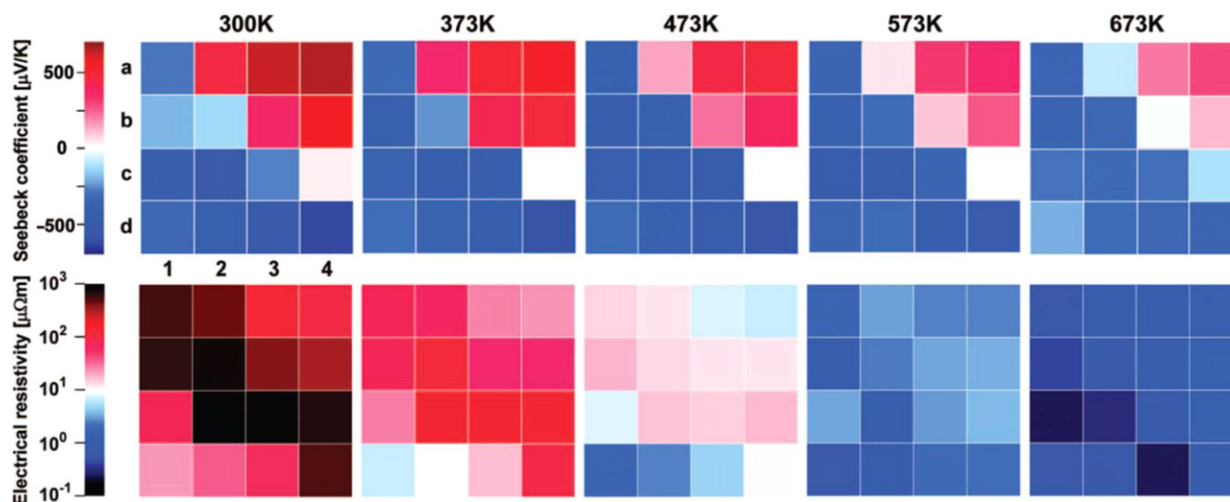
Fig. 6 Compositional dependence of the Seebeck coefficient and electrical resistivity at different temperatures for the Mg-Si-Ge library. A-d and 1–4 refer to various compositional points on the library film (from Watanabe, M., Kita, T., Fukumura, T., et al., 2008. High-throughput screening for combinatorial thin-film library of thermoelectric materials. Journal of Combinatorial Chemistry 10, 175–178.).
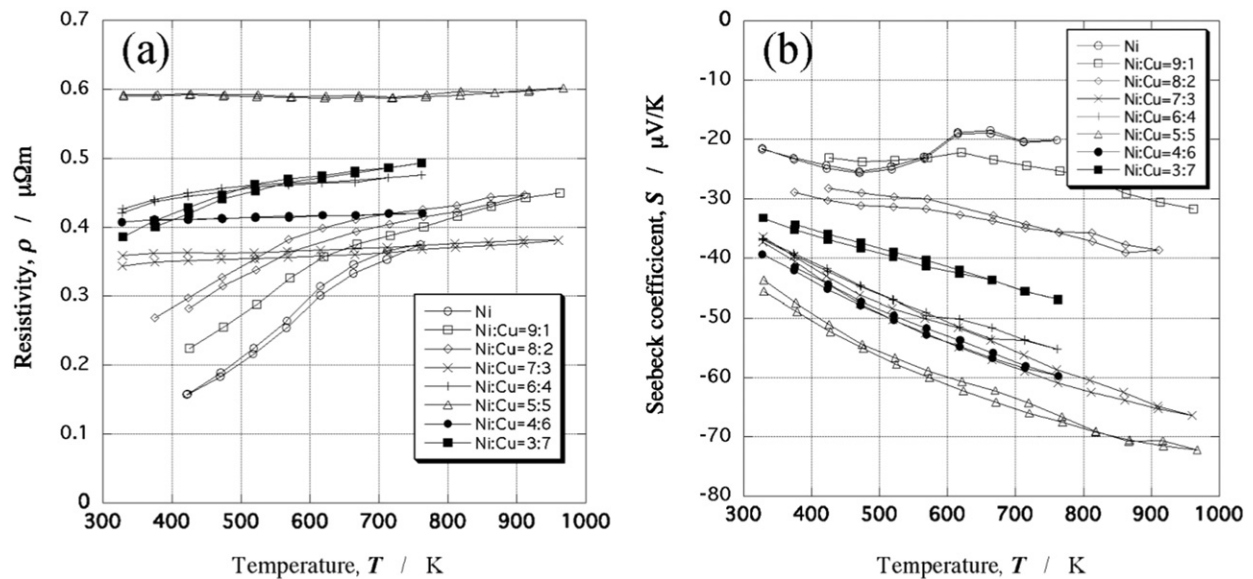
Fig. 7 The temperature dependence of resistivity (a) and Seebeck coefficient (b) of Ni-Cu alloys (from Yamamoto, A., Obara, H., Ueno, K., 2007. Optimization of thermoelectric properties of Ni-Cu based alloy through combinatorial approach. In: Hogan, T.P., Yang, J., Funahashi, R., Tritt, T. (Eds.), MRS Fall Meeting. Boston: Materials Research Society.).
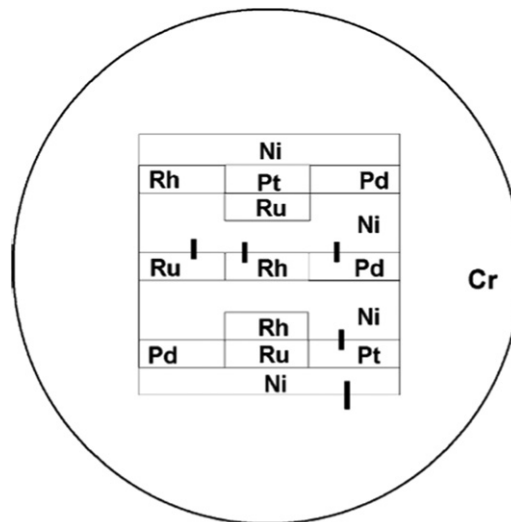
Fig. 8 Schematic diagram of the Ni–Cr–Pd–Pt–Rh–Ru diffusion multiple. The five thick bars mark locations where the composition and thermal conductivity profiles were acquired (from Zheng, X., Cahill, D.G., Krasnochtchekov, P., Averback, R.S., Zhao, J.C., 2007. High-throughput thermal conductivity measurements of nickel solid solutions and the applicability of the Wiedemann-Franz law. Acta Materialia 55, 5177–5185.).

metallurgy techniques involving ball milling of eleven different compositions, followed by spark sintering of powder layers of different compositions to form a bulk sample with a compositional gradient. This bulk library sample was then sliced into thin wafers to expose the compositional gradient. In the second method, discrete compositions were formed in microwells in a graphite sample holder by melting and slicing the pellets. The thermoelectric properties of the $Ni_{1-x}Cu_x$ alloys were measured from 323K to 950K, and the results are shown in **Fig. 7**. In particular, $Ni_{0.7}Cu_{0.3}$ is found to possess a large power factor, 0.012 $Wm^{-1}K^{-2}$ at around 950K (calculable from **Fig. 7(a)** and **(b)**).

In addition to the power factor figure of merit, $S^2\sigma$, the more complete thermoelectric power factor, ZT (equal to $S^2\sigma T/\kappa$) is often desired. Thus, the thermal conductivity, κ, must be determined. Using Ni-based bulk diffusion multiple sample libraries, **Fig. 8**, thermal conductivities of Ni alloys were determined combinatorially by time domain thermoreflectance (TDTR) measurements, with a spatial resolution of about four micrometers, and a sampling rate of three points/sec (Zheng *et al.*, 2007). It is
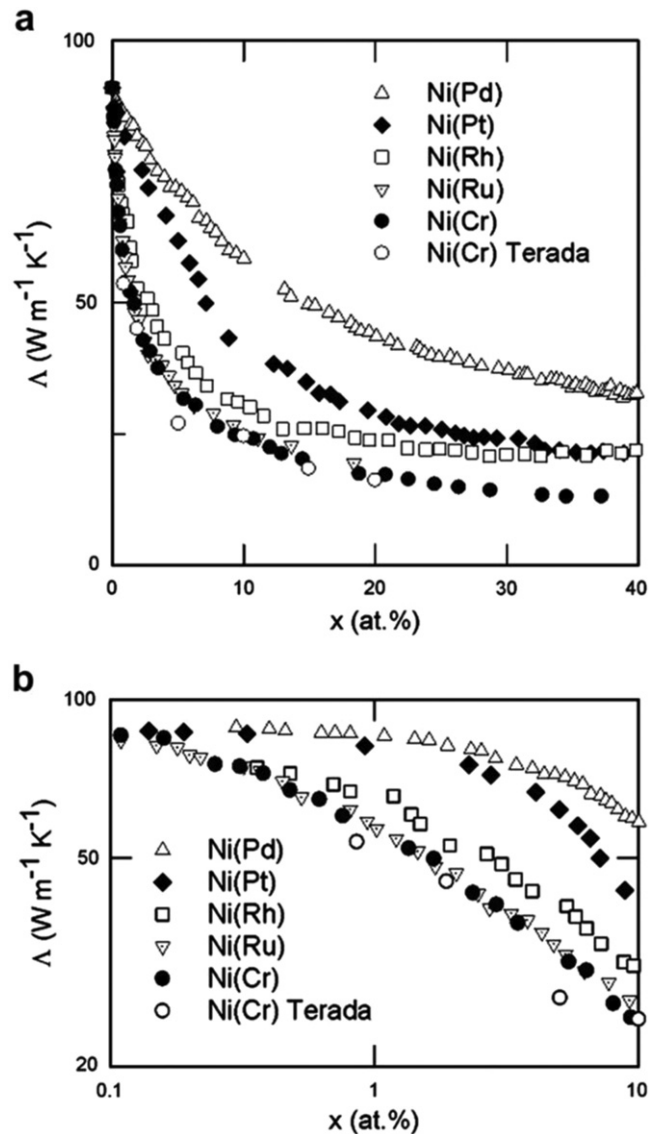
Fig. 9 (a) Composition dependence of the thermal conductivity at room temperature for Ni (Cr), Ni (Pd), Ni (Pt), Ni (Rh) and Ni (Ru) solid solutions. (b) Composition dependence of the thermal conductivity for solute concentrations between 0.1 and 10 at% plotted on a log–log scale. Open triangles, solid diamonds, open squares, dotted triangles and solid circles are data for solutes of Pd, Pt, Rh, Ru and Cr, respectively. Open circles are for earlier non-combinatorial data reported for Ni (Cr) alloys 391 (from Zheng, X., Cahill, D.G., Krasnochtchekov, P., Averback, R.S., Zhao, J.C., 2007. High-throughput thermal conductivity measurements of nickel solid solutions and the applicability of the Wiedemann-Franz law. Acta Materialia 55, 5177–5185.).

also important to note that this data, Fig. 9, shows excellent consistency with non-combinatorially determined values for certain alloys, which were themselves inconsistent with theoretical calculations.

Lithium Battery Anode Materials

Battery powered high technology products are ubiquitous. Since the advent of rechargeable nickel metal hydride (NiMH) batteries enabled environmentally friendly portable electronics, the market for rechargeable batteries has dramatically expanded. Li ion batteries have emerged as the preferred power source for portable electronics, laptops, cell phones, and high performance electric vehicles due to their superior gravimetric and volumetric energy densities, reduced self-discharge, improved cycling capabilities, and thermal stability. State of the art Li ion batteries exhibit remarkable characteristics, with the following properties (maxima) reported: energy storage capacities of 2400 mA h; specific energies of 260 W•h/kg; energy densities of 730 W•h/L; and specific powers of 500 W/kg. Further, they can be cycled 5000 times. (Armand *et al.*, 2020). Typical cells are composed of a graphite anode that intercalates Li ions given off by a $LiCoO_2$ cathode during discharge.

The continued demand for enhanced battery performance has led to the pursuit of improved anode and cathode materials; here we focus on the anode materials. The primary reasons for modifying the anode, often an alloy, is the desire to intercalate more Li atoms per C (graphite) atom, increasing the overall battery capacity, and to reduce the degradation of battery performance as a function of charge/discharge cycles ("cycle fade"). Whereas six C atoms are required to intercalate one Li atom, the same can be accomplished with only four Sn atoms (Fleischauer *et al.*, 2005). The primary source of cycle fade for Li ion battery anodes is the large volume change induced during Li intercalation, which introduces large stresses and therefore fracture of the anode, with a resultant capacity reduction. Two major strategies have been pursued to preserve the capacity while mitigating cycle fade, i.e., placing the active metals in a passive matrix, and the use of amorphous materials. The large compositional phase space represented by anodic materials for Li ion batteries has motivated a number of academic and industrial groups to utilize high throughput methods to identify useful materials. Anode libraries tend to be deposited via sputtering to take advantage of the high quenching rates inherent to that technique. Screening of anode libraries is typically done either through parallel techniques such as imaging (Reddington *et al.*, 1998), **Fig. 10(a)**, the use of automated serial arrays (Fleischauer *et al.*, 2003), **Fig. 10(b)**, or the use of serial electrochemical tests via automated scanning probe measurements (Spong *et al.*, 2003).

In order to increase the resistance of anodes to cycle fade, a great deal of research has been devoted to amorphous alloys containing Si and Sn. However, one difficulty of the sputtering process is subtle run-to-run compositional variations in the libraries, which can add complexity to trends observed when correlating multiple measurements taken on a series of library samples. A novel orbiting sputtering system that allows for the simultaneous deposition of up to five different samples in a single deposition (Fleischauer *et al.*, 2003; Fleischauer and Dahn, 2004), **Fig. 11**, has been developed to circumvent this issue. In a single deposition, libraries for XRD, SEM, gravimetric analysis, and electrochemical cell analysis could be realized.

(a)

(b)
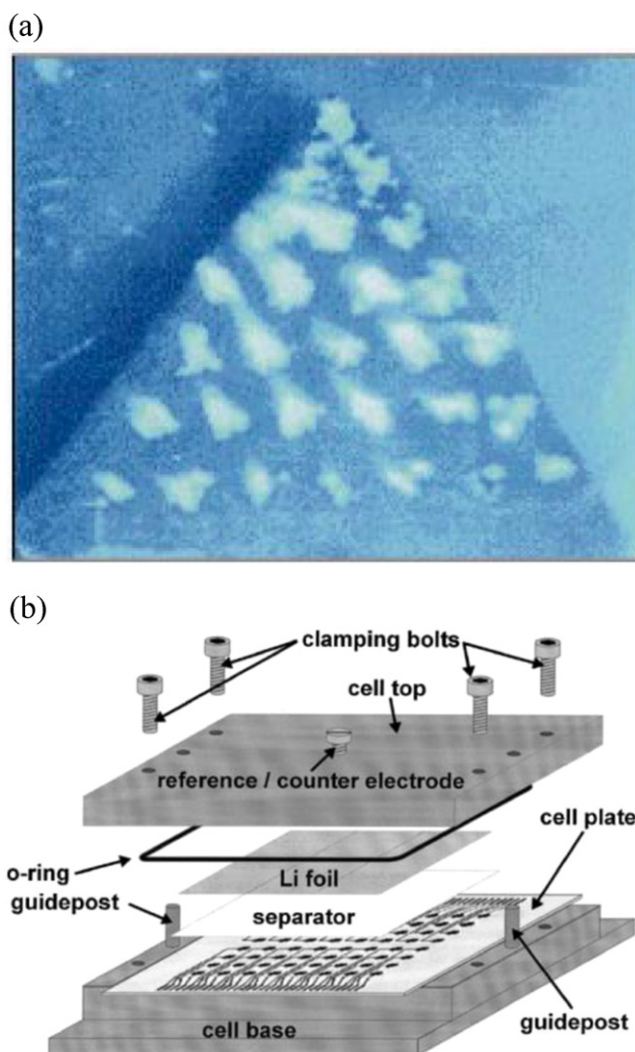
Fig. 10 Example of use of (a) fluorescence libraries (from Reddington, E., Sapienza, A., Gurau, B., *et al.*, 1998. Combinatorial electrochemistry: A highly parallel, optical screening method for discovery of better electrocatalysts. Science 280, 1735–1737.) and (b) apparatus for parallel electrochemical measurements to screen battery materials (from Fleischauer *et al.*, 2003).
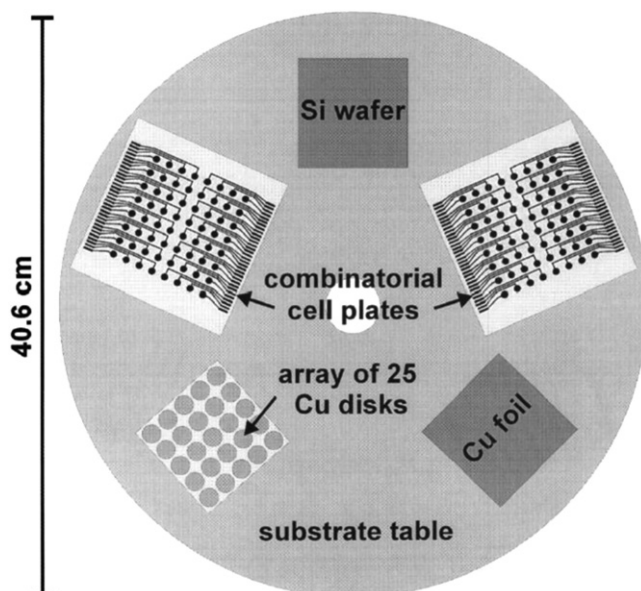
Fig. 11 Schematic of orbital sputtering system (from Fleischauer, M.D., Dahn, J.R., 2004. Combinatorial investigations of the Si-Al-Mn system for Li-ion battery applications. Journal of the Electrochemical Society 151, A1216–A1221.).
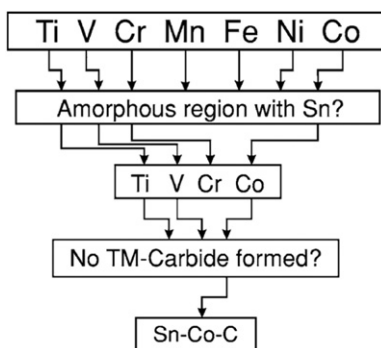
Fig. 12 Roadmap to the selection of the Sn–Co–C system as the best choice among Sn–M–C systems for negative electrodes in Li-ion batteries (from Todd, A.D.W., Mar, R.E., Dahn, J.R., 2006. Combinatorial study of tin-transition metal alloys as negative electrodes for lithium-ion batteries. Journal of the Electrochemical Society 153, A1998–A2005.).

A large amorphous phase region was observed in Si-Al-Mn libraries (Fleischauer and Dahn, 2004), in the same range reported for quenched bulk alloys (Dini and Dunlap, 1986; Inoue et al., 1988). $Si_{0.38}Al_{0.52}Mn_{0.10}$ was identified as exhibiting the best resistance to cycle fade, a gravimetric capacity superior to that of graphite, and a reversible capacity (based on standard Li battery cell type 18650) 40 % higher than for graphite based cells. The predicted resistance to cycle fade was confirmed in experiments using melt spun ribbon (bulk material) (Sun et al., 2008) and was attributed to the formation of a supersaturated solid solution of Si and Mn in α-Al.

A design of experiment approach was used to identify transition metal (TM) additives to Sn-C anodes, which led to the selection of the Sn-Co-C system (Todd et al., 2006), **Fig. 12**. The experimental design focused on selecting TMs that were known to form amorphous compounds with Sn but resisted the formation of carbides. They found that Sn-Co, Sn-Ti, and Sn-V were amorphous for Sn/TM ratios of 1 while small amounts of Carbon resulted in precipitation of the TM carbide. In the particular case of Sn-Co alloys, no Sn precipitation was observed and there was minimal cycle fade observed up to 27 cycles. At least two groups, working with bulk materials, have confirmed the high cycling stability of the Sn-Co-C alloys (Hassoun et al., 2007; Chen et al., 2009).

Sn-Cu compounds, particularly Cu_6Sn_5, have been proposed as potential crystalline anodes, but they exhibit significant cycle fade within the first 50 cycles (Tamura et al., 2002), thought to be due to the large stress associated with the volume during Li intercalation. It has been proposed that nano-sized materials would be better suited to accommodating large volume changes (Winter and Besenhard, 1999). Thorne et. al. showed that C particles that could mitigate grain growth resulting in capacity retention in excess of 90 % (Thorne et al., 2010). The explanation for this behavior is the formation of the Cu_6Sn_5 phase, which becomes the principal Li intercalation material within a C matrix and prevents grain aggregation.

Structural Materials

Metallic Glasses

Metallic Glasses (MGs), solid, amorphous, metal alloys, show great promise for a variety of applications (Khan et al., 2017). Due to their lack of crystalline structure, MGs do not contain crystalline defects such as grain boundaries or dislocations. The lack of dislocations means that there are no slip systems and therefore MGs have excellent mechanical properties such as exceptional hardness and yield strength, as high as 5 GPa (Ashby and Greer, 2006). Also crystalline materials have high energy bonds in and around crystalline defects that can serve as attack sites for corrosion. Because these are absent in MGs, they have very good corrosion resistance (Scully et al., 2011). They also show other promising properties including catalytic activity (Sekol et al., 2013), thermoelectric activity (Nagel, 1978), excellent soft magnetism with (coercivity below 1 A/m) (Tiberto et al., 2007), and high electrical conductivity (Nagel, 1978).

To date only a few thousand alloys have been found to be glass forming. To fully appreciate the range of combinations of properties that are available in MGs, a better understanding of the range of metallic glass chemistries is needed. While it is possible to quench even monatomic metals into a glassy solid (Zhong et al., 2014), alloys with better glass forming ability (GFA) improve manufacturability and therefore their range of applications. Unfortunately it is still quite difficult to predict the GFA of any given alloy chemistry. There are a variety of competing processes and length scales involved in solidification and crystallization that can impact whether a given alloy will form a metallic glass, making successful 1st principles (FP) based simulation of this process quite difficult (Perim et al., 2016). In lieu of these FP models, heuristics, such as Turnbull's rule that MG formers occur around deep eutectics (Turnbull, 1969), have been developed based on a variety of factors including atomic radius ratios and thermodynamic factors. Many such models are referenced and discussed in refs. Khan et al. (2017) and Ren et al. (2018), however none have yet been demonstrated to be globally applicable to all alloys. Further, when these models do fail to completely capture all observations of MG formation, there is often no route to alter them to include these new discoveries.

There is a very large compositional space to search for alloys with good GFA. There are 46 MG-forming elements which have 1035 binary combinations, 15180 ternary combinations and exceedingly more numerous higher dimensional combinations. Examining these higher dimensional combinations is critical, as it has been demonstrated that increasing the number of elements in the alloy improves GFA (Zhang et al., 2015). Discovering new MG forming alloys is even more complicated because simulations suggest, within this vast compositional space, they are actually fairly rare; the model in ref. Ren et al. (2018) predicts that less than 4% of all ternary alloys are glass forming. This large and unpredictable space makes combinatorial methods uniquely suited for MG discovery.

To accelerate the search, there has recently been work on applying traditional combinatorial materials science to this problem (Ding et al., 2014; Perim et al., 2016). Ren et al. (2018) describes a study coupling combinatorial thin-films growth, rapid x-ray diffraction screening (described below), and machine learning to accelerate the search for new metallic glasses by 2–3 orders of magnitude. The outline of this research paradigm is illustrated in **Fig. 13**. Additive manufacturing has also been leveraged for rapid synthesis of bulk metallic glasses (Tsai and Flores, 2016).

Several methods have also been used for rapidly screening MG alloys for functional properties. Nanoindentation (NI) is a well-studied method for characterizing mechanical properties in many materials, including metallic glasses (Burgess and Ferry, 2009; Tsai and Flores, 2016). One of the main advantages of NI is that the indentation is very shallow, making it compatible with thin films combinatorial libraries. NI has previously been demonstrated as a high-throughput tool (Dwivedi et al., 2008). Other more exotic high-throughput measurements, such as the one shown in **Fig. 14**, have been developed specifically for the study of metallic glasses involving the creation of 3-dimensional nanostructures (Ding et al., 2014; Hasan and Kumar, 2017). Various high-throughput corrosion screening tools have also been developed, either using a scanning droplet cell for localized electrochemical corrosion, shown in **Fig. 15**, (Joress et al., 2020) or using optical methods to compare corrosion effects across a library (Kotoka et al., 2016).

High Entropy Alloys

The past 10 years have seen significant interest in the study of so-called high entropy alloys (HEA) or multiple principal component alloys in the scientific literature (Miracle and Senkov, 2017). A HEA can be defined as an alloy that contains 3 or more principal components, generally combined in equiatomic or near equiatomic proportions, and typically forms in a simple solid solution structure. A host of HEA systems have been investigated for their mechanical, magnetic, and corrosion resistant properties among others (Tsai and Yeh, 2014). The solid solution nature of HEAs potentially provides a means to continuously vary their properties by compositional substitution; HEAs are therefore a natural system for combinatorial/high-throughput exploration as highlighted in a recent paper by Miracle et al. (2014), and a number of recent studies were discussed in a recent review by Li et al. (2018). Many of the characterization techniques described elsewhere in this review can be used to investigate the physical properties of these alloys, although new tools are still required to expedite the rate of screening for bulk properties (e.g., tensile testing). Below we discuss the synthesis challenges associated with depositing a large number of elements as bulk and thin film samples.

Because many applications of HEAs are in structural applications (e.g. high temperature turbine blades) combinatorial work in this field has focused on development of bulk alloys, although numerous thin films studies have also been reported. Within the field, so-called Cantor Alloys (e.g. transition metal based HEAs) are by far the most thoroughly explored systems, though more recently there has been work in refractory HEAs. Pradeep et al. (2015) developed a combinatorial induction melting
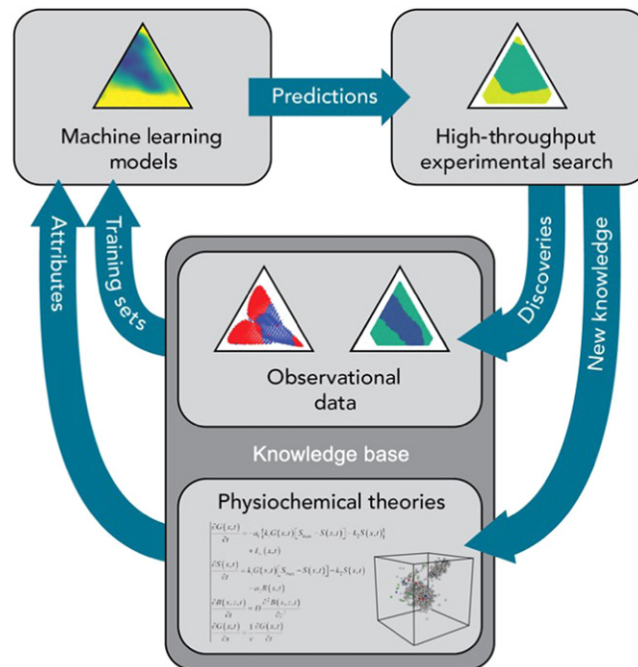
Fig. 13 Schematic depiction of a paradigm for rapid and guided discovery of materials through iterative combination of ML with HiTp experimentation (from Ren *et al.*, 2018).
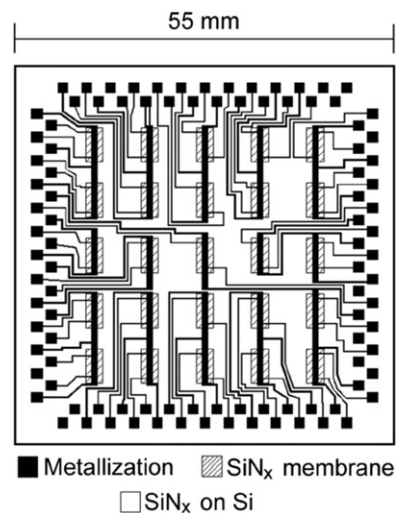
Fig. 14 Schematic of the parallel nano-scanning calorimeter (from McCluskey and Vlassak, 2011).

technique to investigate HEAs. Blown powder Laser engineered net-shaping (LENS) additive manufacturing systems are more regularly applied for combinatorial alloy investigations (Dippo *et al.*, 2021; Kunce *et al.*, 2014; Chaudhary *et al.*, 2020; Moorehead *et al.*, 2020). In these specialized systems, a multi-hopper powder feed system is used to vary the composition of the source material, which is then blown onto the workpiece, coincident with a focused laser, enabling spot by spot compositional control, as shown in **Fig. 16**. Recently Agrawal *et al.* (2020), Weaver *et al.* (2021) used a powder bed system to perform a combinatorial investigation of the role of AM processing parameters, laser power, scanning speed, and hatch spacing on the hardness and density of 316L stainless steel and Ni 625 respectively; similar methods could be used for screening AM printed libraries.

Combinatorial investigations using physical vapor deposition, typically magnetron sputtering, are largely performed using the types of techniques discussed above. The difficulty comes in accommodating the systematic variation in deposition systems with a limited number of deposition sources (3 sources is typical for many chambers). Ruiz-Yi *et al.* (2016) employed AlFeNiTiVZr,
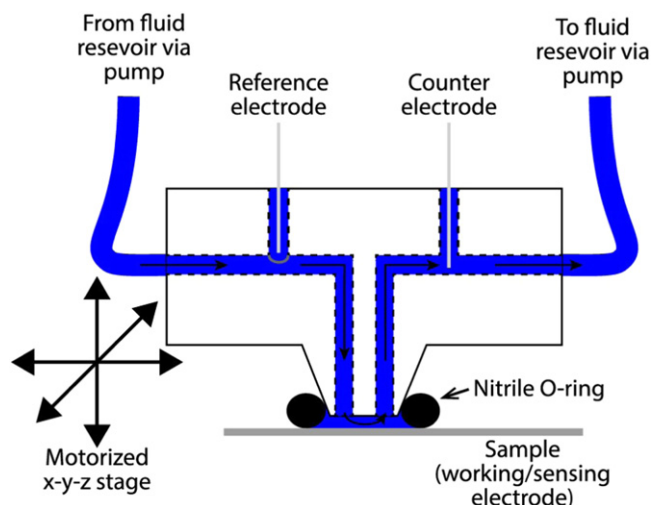
Fig. 15 Schematic showing the scan head of the SDC. The electrolyte flows through the scan head passing by the reference and counter electrodes as illustrated. The scan head is mounted on a motorized Z stage to enable contact of the scan head with the sample. The sample is mounted underneath the scan head on a motorized x-y stage to allow for rasteringof the scan head over the sample (from Joress *et al.*, 2020).
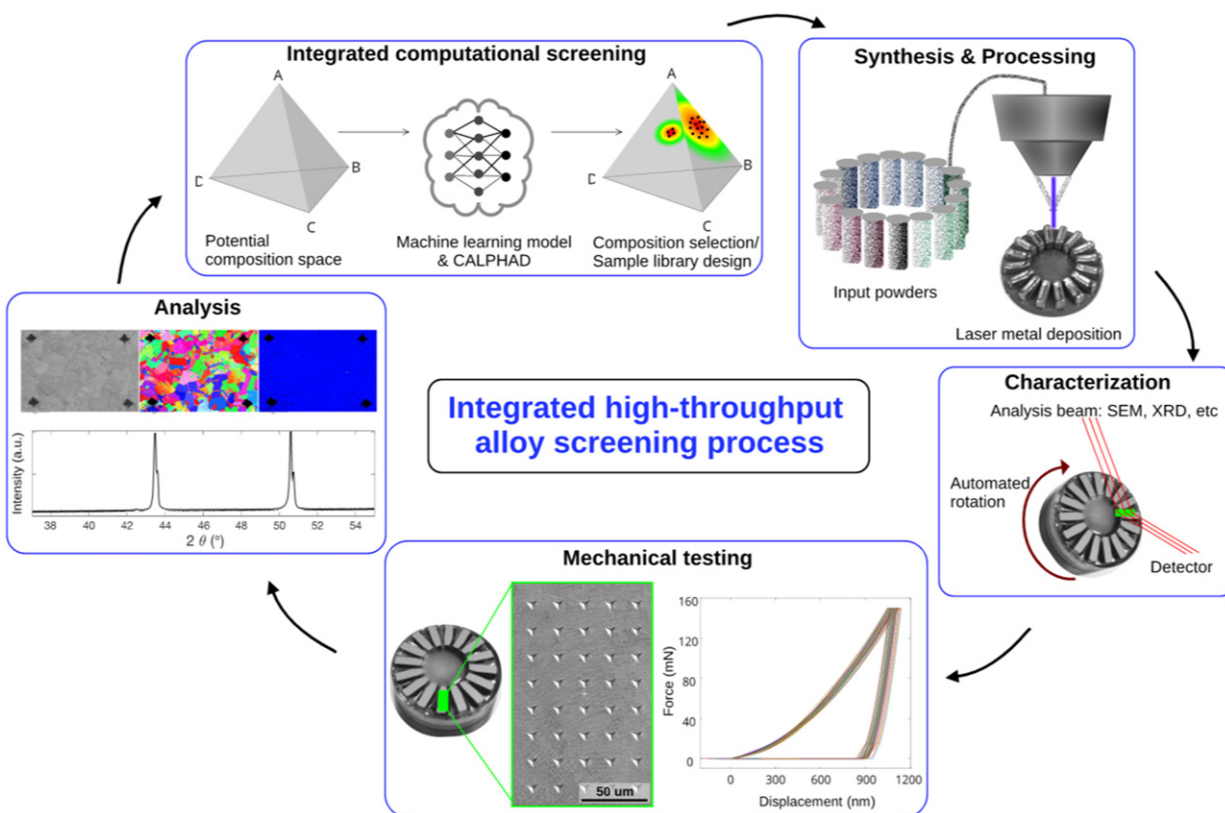
Fig. 16 Illustration of the steps incorporated into the integrated High-Throughput Rapid Experimental Alloy Development (HT-READ) methodology. Clockwise from top left, computational screeningutilizing CALPHAD and machine learning model provide recommendations for sample library compositions. Then samples are synthesized, processed, characterized, tested, and analyzed in an automated, high-throughput fashion. New data is utilized to improve subsequent screening and design (from Dippo *et al.*, 2021).

CuFeNiTiVZr, and MoFeNiTiVZr alloy targets to form an $(Al_{1-x-y}Cu_xMo_y)FeNiTiVZr$ pseudo-ternary composition spread. A single cathode method was demonstrated by Kauffmann et. al. in which a single target was composed of 5 wedges of different elements, as shown in **Fig. 17**, that had been bonded together and deposited in such a way to generate a natural composition gradient (Kauffmann *et al.*, 2017). Of course there are also examples where larger numbers of sources are employed in order to obtain
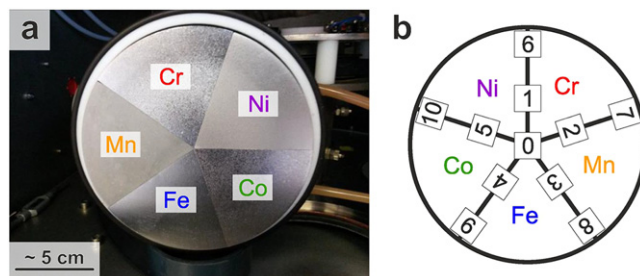
Fig. 17 (a) 5 partmagnetron sputter target and (b) scheme of the placement of eleven Si substrates (no. 0 to 10) underneath the target sections (from Kauffman et al., 2017).

variation over more elements (Marshal et al., 2019). The current state of the art composition spread synthesis techniques beyond ternary and pseudo-ternary libraries, however, are limited in their ability to systematically and fully sample the 5 + dimensional composition space HEAs exist in. Rather, these methods create libraries on complex, lower dimensional surfaces through this space. Pad-by-pad techniques are available but are much slower than composition spread deposition and can only sparsely sample the composition space. Furthermore, in both instances, processing space is frequently addressed through the use of a thermal gradient during annealing across the wafer, which removes an additional degree of freedom normally taken by composition. Thus new rapid synthesis techniques that can efficiently probe composition – processing space for alloys containing 5 or more components, perhaps guided by AI agents, are required.

High-Throughput Mapping of Phase Diagrams and Shape Memory Alloys

Mapping of compositional phase diagrams is an integral part of any materials exploration effort. Not surprisingly, combining information regarding distribution of structural phases across phase diagrams with mapping of functional properties represents a particularly powerful way to rapidly identify new compositions and compounds with enhanced physical properties. In the fields of metallurgy and ceramics, mapping binary and higher-order phase diagrams through bulk compound synthesis is a traditional and critical task. However, despite concerted global efforts by materials scientists, a large fraction of all possible ternary and multinary alloys remain experimentally unexplored. In fact, the history of materials science is paved with efforts to understand and map phase diagrams. The high-throughput thin film library approach, combined with scanning XRD experiments represents a tremendous opportunity, as had been recognized as far back as 55 years ago (Kennedy et al., 1965). Bulk high-throughput efforts such as diffusion multiples (Zhao, 2006) and directed laser deposition (Collins, 2004) have also been successfully implemented to map structural phases in composition gradient samples. The synchrotron XRD mapping exercise is particularly useful when combined with x-ray fluorescence for composition determination (Gregoire et al., 2009; Isaacs et al., 1998).

Given the speed with which structural data can be acquired, for example the aforementioned synchrotron experiments, the rapid analysis of large amounts of raw XRD data becomes a challenge. There have been a number of efforts directed at developing algorithms that allow rapid identification of key trends and features in diffraction data taken across multiphase CCS libraries, and subsequent attribution of such data to individual phases (Long et al., 2009; Barr et al., 2004). By performing cluster analysis, similar diffraction patterns, even among hundreds of spectra, can be rapidly identified. Similar XRD patterns usually indicate the presence of similar phases in a particular composition region. Thus, one goal of these algorithms is to automatically identify mixtures of crystallographic phases, even when significant diffraction peak shifting, for example due solid solution substitutional effects, is present. These analysis techniques are extremely useful in directly and visually delineating the composition-structure-property relationships of materials systems. Many of the algorithms developed for handling large amount of XRD data are also applicable to rapid analysis of other spectra such as Raman, XPS, and FTIR data (Jain et al., 2012).

As a general comment, computational combinatorial approaches have recently received much attention with the arrival of the Materials Genome Initiative (MGI). To take advantage of the power of high-throughput methodologies, an integrated strategy combining computational methods with rapid experimental verification work is required. Thus going forward, the challenge for combinatorial methodology is the effective coupling of synthesis, characterization and theory (Curtarolo et al., 2012). Further, machine learning can help reduce the time needed to scan libraries through a closed-loop approach in addition to data fusion with additional characterization modalities, illustrated in **Fig. 18**. (Kusne et al., 2020).

Accurate structural phase mapping can directly facilitate rapid discovery of functional materials whose interesting properties are derived from phase transformations. Morphotropic phase boundary piezoelectrics, discussed in Section "Magnetic Materials", are a good example. Further, SMAs undergo structural transitions as a result of martensitic phase transformations, going from high temperature, higher symmetry parent phases to low temperature, lower symmetry martensites. The technological applications of many SMAs depend on operating the alloys in the temperature range of their phase transformations; for example, superelasticity, a property that derives from stress-induced transformations, can be used to accommodate large strains in mechanical framework for
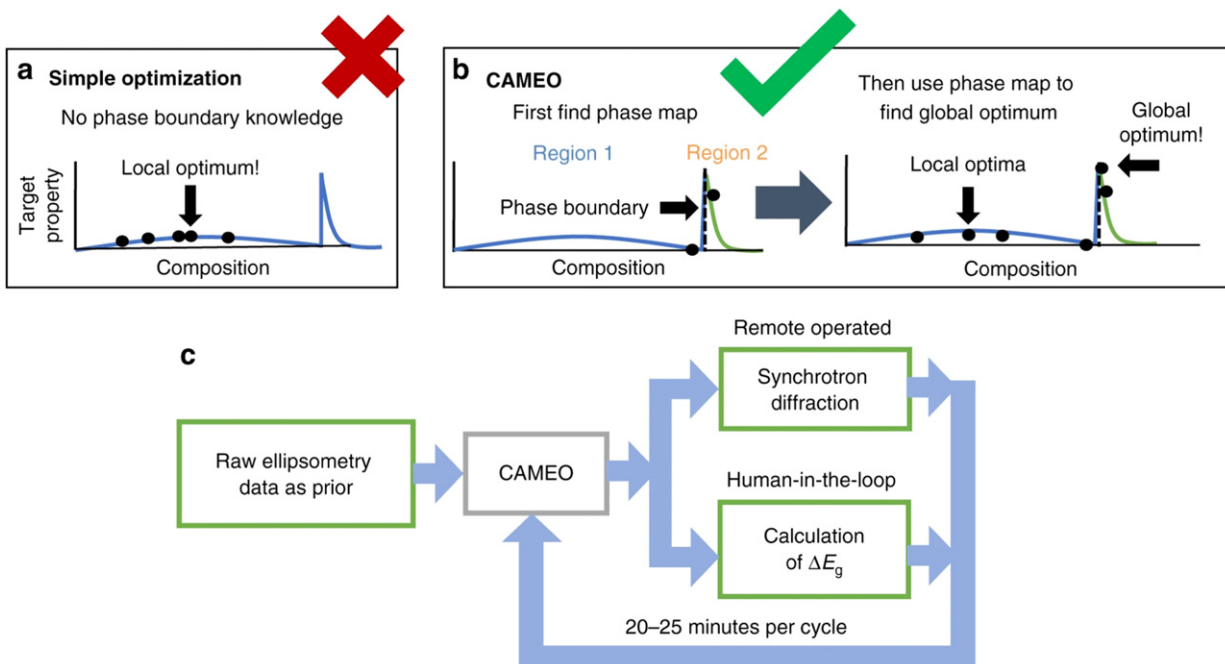
Fig. 18 (a) Simple optimization seeks to identify the property optimum with a mixture of exploration and exploitation without knowledge of the composition-structure-property (CSP) relationship. These methods are more likely to get caught in local optima. (b) The phase-map-informed optimization scheme exploits CSP relationship by recognizing that the property is dependent on phase, thus including phase mapping in the search for the optimum. (i) Phase-mapping steps and (ii) materials optimization step that exploits knowledge of the phase boundaries. This allows a search for phase region dependent optima. (c) The Ge–Sb–Te CAMEO workflow began with incorporating raw ellipsometry data as a phase-mapping prior. On each iteration, CAMEO selects a material to measure for X-ray diffraction and concurrently requests an expert to calculate ΔE_g for that material. Each cycle takes 20–25 min (from Kusne *et al.*, 2020).

a variety of body or room-temperature applications including dental braces, peripheral vascular stents, and eyeglass frames (Lagoudas, 2008). A variety of high-throughput studies have been performed (Cui *et al.*, 2006; Zarnetta *et al.*, 2010).

Other methods of mapping phase diagrams of SMAs involve their mechanical properties. Since they are mechanically soft in their martensitic state, nanoindentation mapping of elastic modulus has been effectively used to identify martensite composition regions (Dwivedi *et al.*, 2008). Another method for detection of the martensitic transition is through implementation of arrays of cantilevers, since the change in the elastic modulus of the film deposited atop the cantilever as a result of the martensitic transition results in an abrupt deflection (Takeuchi *et al.*, 2003). Indeed, cantilever arrays have served as a versatile combinatorial platform for mapping a variety of mechanical properties such as film stresses, glass transitions, and fatigue (Ludwig *et al.*, 2005; Burger *et al.*, 2011; Kim *et al.*, 2008). Finally, other dense MEMS sensor arrays, such as microhotplates for nanocalorimetry and gas sensors, have been very useful in high throughput measurements (McCluskey and Vlassak, 2011; Semancik, 2003). **Fig. 2** illustrates a nano-calorimeter array device.

Appendix (List Of Abbreviations)

CCS Continuous composition spread.
CMOS Complementary metal oxide semiconductor.
C-V Capacitance-voltage.
CVD Chemical vapor deposition.
FTIR Fourier transform infrared spectroscopy.
ITRS International Technology Roadmap for Semiconductors.
I-V Current-voltage.
IR Infrared.
MEMS Microelectromechanical systems.
MOKE Magnetic-optical Kerr effect.
NMOS n-channel metal oxide semiconductor.
PCM Phase change material.

PLD   Pulsed laser deposition.
PMOS   p-channel metal oxide semiconductor.
RE   Rare earth.
RF   Radio frequency.
RT   Room temperature.
SMA   Shape memory alloy.
SQUID   Superconducting quantum interference device.
TDTR   Time domain thermoreflectance.
TM   Transition metal.
WDS   Wavelength dispersive spectroscopy.
XPS   X-ray photoemission spectroscopy.
XRD   X-ray diffraction.

References

Agrawal, A.K., Meric De Bellefon, G., Thoma, D., 2020. High-throughput experimentation for microstructural design in additively manufactured 316L stainless steel. Materials Science and Engineering A 793. 139841.

Alshareef, H.N., Choi, K., Wen, H.C., et al., 2006. Composition dependence of the work function of Ta1-xAlxNy metal gates. Applied Physics Letters 88. 072108.

Armand, M., Axmann, P., Bresser, D., et al., 2020. Lithium-ion batteries – Current state of the art and anticipated developments. Journal of Power Sources 479. 228708.

Aronova, M.A., 2004. Combinatorial investigation of magnetic materials. University of Maryland.

Ashby, M., Greer, A., 2006. Metallic glasses as structural materials. Scripta Materialia 54, 321–326.

Barber, Z.H., Blamire, M.G., 2008. High throughput thin film materials science. Materials Science and Technology 24, 757–770.

Barr, G., Dong, W., Gilmore, C.J., 2004. PolySNAP: A computer program for analysing high-throughput powder diffraction data. Journal of Applied Crystallography 37, 658–664.

Boettcher, A., Haase, G., Thun, R., 1955. STRUKTURUNTERSUCHUNG VON MEHRSTOFFSYSTEMEN DURCH KINEMATISCHE ELEKTRONENBEUGUNG. Zeitschrift Fur Metallkunde 46, 386–400.

Boyce, B.L., Uchic, M.D., 2019. Progress toward autonomous experimental systems for alloy development. MRS Bulletin 44, 273–280.

Bozorth, R.M., 1993. Ferromagnetism. New Jersey: Wiley-IEEE Press.

Burger, S., Eberl, C., Siegel, A., Ludwig, A., Kraft, O., 2011. A novel high-throughput fatigue testing method for metallic thin films. Science and Technology of Advanced Materials 12.(7).

Burgess, T., Ferry, M., 2009. Nanoindentation of metallic glasses. Materials Today 12, 24–32.

Chang, K.S., Green, M.L., Suehle, J., et al., 2006. Combinatorial study of Ni-Ti-Pt ternary metal gate electrodes on HfO$_2$ for the advanced gate stack. Applied Physics Letters 89. 142108.

Chang, K.S., Green, M.L., Hattrick-Simpers, J.R., et al., 2008. Determination of work functions in the Ta1-xAlxNy/HfO$_2$ advanced gate stack using combinatorial methodology. IEEE Transactions on Electron Devices 55, 2641–2647.

Chaudhary, R.P., Gandha, K.H., Meng, F., et al., 2020. Development of mischmetal–Fe–Co–B permanent magnet alloys via high-throughput methods. ACS Combinatorial Science 22, 248–254.

Chen, Z.X., Qian, J.F., Ai, X.P., Cao, Y.H., Yang, H.X., 2009. Preparation and electrochemical performance of Sn-Co-C composite as anode material for Li-ion batteries. Journal of Power Sources 189, 730–732.

Chisholm, B.J., Webster, D.C., 2007. The development of coatings using combinatorial/high throughput methods: A review of the current status. Journal of Coatings Technology and Research 4, 1–12.

Collins, P.C., 2004. A Combinatorial Approach to the Development of Compoisition-Microstructure-Property Relationships in Titanium Alloys Using Directed Laser Deposition. Ohio State University.

Cui, J., Chu, Y.S., Famodu, O.O., et al., 2006. Combinatorial search of thermoelastic shape-memory alloys with extremely small hysteresis width. Nature Materials 5, 286–290.

Curtarolo, W. S, S., Hart, G.L.W., Jahnatek, M., et al., W. S. et al., 2012. AFLOW: An automatic framework for high-throughput materials discovery. Computational Materials Science 58, 218–226.

Dellamorte, J.C., Barteau, M.A., Lauterbach, J., 2009. Opportunities for catalyst discovery and development: Integrating surface science and theory with high throughput methods. Surface Science 603, 1770–1775.

Ding, S., Liu, Y., Li, Y., et al., 2014. Combinatorial development of bulk metallic glasses. Nature Materials 13, 494–500.

Dini, K., Dunlap, R.A., 1986. The Relationship of the Quasi-crystalline Icosahedral Phase to the Amorphous Structure in Rapidly quenched AL-MN-SI and AL-FE-SI Alloys. Journal of Physics F-Metal Physics 16, 1917–1925.

Dippo, O.F., Kaufmann, K.R., Vecchio, K.S. 2021. High-throughput rapid experimental alloy development (HT-READ). arXiv preprint arXiv:2102. 06180.

Dwivedi, A., Wyrobek, T.J., Warren, O.L., et al., 2008. High-throughput screening of shape memory alloy thin-film spreads using nanoindentation. Journal of Applied Physics 104. 073501.

Famodu, O.O., Hattrick-Simpers, J., Aronova, M., et al., 2004. Combinatorial investigation of ferromagnetic shape-memory alloys in the Ni-Mn-Al ternary system using a composition spread technique. Materials Transactions 45, 173–177.

Fleischauer, M.D., Dahn, J.R., 2004. Combinatorial investigations of the Si-Al-Mn system for Li-ion battery applications. Journal of the Electrochemical Society 151, A1216–A1221.

Fleischauer, M.D., Hatchard, T.D., Rockwell, G.P., et al., 2003. Design and testing of a 64-channel combinatorial electrochemical cell. Journal of the Electrochemical Society 150, A1465–A1469.

Fleischauer, M.D., Hatchard, T.D., Bonakdarpour, A., Dahn, J.R., 2005. Combinatorial investigations of advanced Li-ion rechargeable battery electrode materials. Measurement Science & Technology 16, 212–220.

Fukumura, T., Ohtani, M., Kawasaki, M., et al., 2000. Rapid construction of a phase diagram of doped Mott insulators with a composition-spread approach. Applied Physics Letters 77, 3426–3428.

Green, M.L., Takeuchi, I., Hattrick-Simpers, J.R., 2013. Applications of high throughput (combinatorial) methodologies to electronic, magnetic, optical, and energy-related materials. Journal of Applied Physics 113. 231101.

Gregoire, J.M., Dale, D., Kazimirov, A., Disalvo, F.J., Bruce van Dover, R., 2009. High energy x-ray diffraction/x-ray fluorescence spectroscopy for high-throughput analysis of composition spread thin films. Review of Scientific Instruments 80.

Hanak, J.J., Gittleman, J.I., 1972. Iron-nickel-silica ferromagnetic cermets. AIP Conference Proceedings. 961–965.

Hasan, M., Kumar, G., 2017. High-throughput drawing and testing of metallic glass nanostructures. Nanoscale 9, 3261–3268.

Hassoun, J., Mulas, G., Panero, S., Scrosati, B., 2007. Ternary Sn-Co-CLi-ion battery electrode material prepared by high energy ball milling. Electrochemistry Communications 9, 2075–2081.

Ielmini, D., Lacaita, A.L., 2011. Phase change materials in non-volatile storage. Materials Today 14, 600–607.

Inoue, A., Bizen, Y., Kimura, H.M., Masumoto, T., Sakamoto, M., 1988. Compositional range, thermal-stability, hardness and electrical-resistivity of amorphous-alloys in AL-SI (or GE)-transition metal systems. Journal of Materials Science 23, 3640–3647.

Isaacs, E.D., Marcus, M., Aeppli, G., et al., 1998. Synchrotron x-ray microbeam diagnostics of combinatorial synthesis. Applied Physics Letters 73, 1820–1822.

Jain, A., Hautier, G., Moore, C., et al., 2012. A computational investigation of Li9M3 (P2O7) (3) (PO4) (2) (M = V, Mo) as Cathodes for Li ion batteries. Journal of the Electrochemical Society 159, A622–A633.

Joress, H., Decost, B.L., Sarker, S., et al., 2020. A high-throughput structural and electrochemical study of metallic glass formation in Ni–Ti–Al. ACS Combinatorial Science 22, 330–338.

Kanatzidis, M.G., Mahanti, S.D., Hogan, T.P., 2003. Chemistry, Physics, and Materials Science of Thermoelectric Materials: Beyond Bismuth Telluride. New York, NY: Plenum Publishers.

Kauffmann, A., Stüber, M., Leiste, H., et al., 2017. Combinatorial exploration of the high entropy alloy system Co-Cr-Fe-Mn-Ni. Surface and Coatings Technology 325, 174–180.

Kennedy, K., Stefansky, T., Davy, G., Zackay, V.F., Parker, E.R., 1965. Rapid method for determining ternary-alloy phase diagrams. Journal of Applied Physics 36. 3808.

Khan, M.M., Nemati, A., Rahman, Z.U., et al., 2017. Recent advancements in bulk metallic glasses and their applications: A review. Critical Reviews in Solid State and Materials Sciences 43, 233–268.

Kim, H.-J., Han, J.-H., Kaiser, R., Oh, K.H., Vlassak, J.J., 2008. High-throughput analysis of thin-film stresses using arrays of micromachined cantilever beams. Review of Scientific Instruments 79.

Kirsten, G., Maier, W.F., 2004. Strategies for the discovery of new catalysts with combinatorial chemistry. Applied Surface Science 223, 87–101.

Koinuma, H., Takeuchi, I., 2004. Combinatorial solid-state chemistry of inorganic materials. Nature Materials 3, 429–438.

Kotoka, R., Konchady, M., Ramakrishnan, G., et al., 2016. High throughput corrosion screening of Mg-Zn combinatorial material libraries. Materials & Design 108, 42–50.

Kunce, I., Polanski, M., Bystrzycki, J., 2014. Microstructure and hydrogen storage properties of a TiZrNbMoV high entropy alloy synthesized using Laser Engineered Net Shaping (LENS). International Journal of Hydrogen Energy 39, 9904–9910.

Kusne, A.G., Yu, H., Wu, C., et al., 2020. On-the-fly closed-loop materials discovery via Bayesian active learning. Nature Communications 11. 5966.

Kyrsta, S., Cremer, R., Neuschutz, D., et al., 2001. Characterization of Ge-Sb-Te thin films deposited using a composition-spread approach. Thin Solid Films 398, 379–384.

Lagoudas, D.C., 2008. Shape Memory Alloys: Modeling and Engineering Applications. New York: Springer.

Li, Z., Ludwig, A., Savan, A., Springer, H., Raabe, D., 2018. Combinatorial metallurgical synthesis and processing of high-entropy alloys. Journal of Materials Research 33, 3156–3169.

Long, C.J., Bunker, D., Li, X., Karen, V.L., Takeuchi, I., 2009. Rapid identification of structural phases in combinatorial thin-film libraries using x-ray diffraction and non-negative matrix factorization. Review of Scientific Instruments 80.

Ludwig, A., Cao, J., Brugger, J., Takeuchi, I., 2005. MEMS tools for combinatorial materials processing and high-throughput characterization. Measurement Science & Technology 16, 111–118.

Maier, W.F., Stoewe, K., Sieg, S., 2007. Combinatorial and high-throughput materials science. Angewandte Chemie-International Edition 46, 6016–6067.

Marshal, A., Pradeep, K.G., Music, D., et al., 2019. Combinatorial evaluation of phase formation and magnetic properties of FeMnCoCrAl high entropy alloy thin film library. Scientific Reports 9. 7864.

Matsumoto, Y., Koinuma, H., Hasegawa, T., et al., 2003. Combinatorial investigation of spintronic materials. MRS Bulletin 28, 734–739.

McCluskey, P.J., Vlassak, J.J., 2011. Glass transition and crystallization of amorphous Ni-Ti-Zr thin films by combinatorial nano-calorimetry. Scripta Materialia 64, 264–267.

Miracle, D.B., Senkov, O.N., 2017. A critical review of high entropy alloys and related concepts. Acta Materialia 122, 448–511.

Miracle, D.B., Miller, J.D., Senkov, O.N., Woodward, C., Uchic, M.D., Tiley, J., 2014. Exploration and development of high entropy alloys for structural applications. Entropy 16.

Moorehead, M., Bertsch, K., Niezgoda, M., et al., 2020. High-throughput synthesis of Mo-Nb-Ta-W high-entropy alloys via additive manufacturing. Materials & Design 187. 108358.

Nagel, S.R., 1978. Thermoelectric power and resistivity in a metallic glass. Physical Review Letters 41, 990–993.

Park, C.S., Cho, B.J., Kwong, D.L., 2003. An integratable dual metal gate CMOS process using an ultrathin aluminum nitride buffer layer. IEEE Electron Device Letters 24, 298–300.

Perim, E., Lee, D., Liu, Y., et al., 2016. Spectral descriptors for bulk metallic glasses based on the thermodynamics of competing crystalline phases. Nature Communications 7. 12315.

Potyrailo, R.A., Mirsky, V.M., 2008. Combinatorial and high-throughput development of sensing materials: The first 10 years. Chemical Reviews 108, 770–813.

Pradeep, K.G., Tasan, C.C., Yao, M.J., et al., 2015. Non-equiatomic high entropy alloys: Approach towards rapid alloy screening and property-oriented design. In: Materials Science and Engineering A, 648. pp. 183–192.

Reddington, E., Sapienza, A., Gurau, B., et al., 1998. Combinatorial electrochemistry: A highly parallel, optical screening method for discovery of better electrocatalysts. Science 280, 1735–1737.

Ren, F., Ward, L., Williams, T., et al., 2018. Accelerated discovery of metallic glasses through iteration of machine learning and high-throughput experiments. Sci Adv. 4.

Ruiz-Yi, B., Bunn, J.K., Stasak, D., et al., 2016. The different roles of entropy and solubility in high entropy alloy stability. ACS Combinatorial Science 18, 596–603.

Scully, J.R., Gebert, A., Payer, J.H., 2011. Corrosion and related mechanical properties of bulk metallic glasses. Journal of Materials Research 22, 302–313.

Sekol, R.C., Kumar, G., Carmo, M., et al., 2013. Bulk metallic glass micro fuel cell. Small 9 (12), 2081–2085.

Semancik, S. (Ed.), 2003. Temperature-Dependent Materials Research With Micromachined Array Platforms. New York: Marcel Dekker, Inc.

Shimizu, R., Kobayashi, S., Watanabe, Y., Ando, Y., Hitosugi, T., 2020. Autonomous materials synthesis by machine learning and robotics. APL Materials 8.

Spong, A.D., Vitins, G., Guerin, S., et al., 2003. Combinatorial arrays and parallel screening for positive electrode discovery. Journal of Power Sources 119, 778–783.

Sun, Z.B., Wang, X.D., Li, X.P., et al., 2008. Electrochemical properties of melt-spun Al-Si-Mn alloy anodes for lithium-ion batteries. Journal of Power Sources 182, 353–358.

Takeuchi, I., Van Dover, R.B., Koinuma, H., 2002. Combinatorial synthesis and evaluation of functional inorganic materials using thin-film techniques. MRS Bulletin 27, 301–308.

Takeuchi, I., Famodu, O.O., Read, J.C., et al., 2003. Identification of novel compositions of ferromagnetic shape-memory alloys using composition spreads. Nature Materials 2, 180–184.

Tamura, N., Ohshita, R., Fujimoto, M., et al., 2002. Study on the anode behavior of Sn and Sn-Cu alloy thin-film electrodes. Journal of Power Sources 107, 48–55.

Thorne, J.S., Sanderson, R.J., Dahn, J.R., Dunlap, R.A., 2010. Combinatorial study of the Sn-Cu-C system for Li-ion battery negative electrode materials. Journal of the Electrochemical Society 157, A1085–A1091.

Tiberto, P., Baricco, M., Olivetti, E., Piccin, R., 2007. Magnetic properties of bulk metallic glasses. Advanced Engineering Materials 9, 468–474.

Todd, A.D.W., Mar, R.E., Dahn, J.R., 2006. Combinatorial study of tin-transition metal alloys as negative electrodes for lithium-ion batteries. Journal of the Electrochemical Society 153, A1998–A2005.

Tsai, M.-H., Yeh, J.-W., 2014. High-entropy alloys: A critical review. Materials Research Letters 2, 107–123.

Tsai, P., Flores, K.M., 2016. High-throughput discovery and characterization of multicomponent bulk metallic glass alloys. Acta Materialia 120, 426–434.

Turnbull, D., 1969. Under what conditions can a glass be formed? Contemporary Physics 10, 473–488.

Watanabe, M., Kita, T., Fukumura, T., et al., 2008. High-throughput screening for combinatorial thin-film library of thermoelectric materials. Journal of Combinatorial Chemistry 10, 175–178.

Weaver, J.S., Pintar, A.L., Beauchamp, C., et al., 2021. Demonstration of a laser powder bed fusion combinatorial sample for high-throughput microstructure and indentation characterization. Materials & Design 209, 109969. ISSN 0264-1275, https://doi.org/10.1016/j.matdes.2021.109969.

Winter, M., Besenhard, J.O., 1999. Electrochemical lithiation of tin and tin-based intermetallics and composites. Electrochimica Acta 45, 31–50.

Wong-Ng, W., Yan, Y., Otani, M., et al., 2014. High throughput screening tools for thermoelectric materials. Journal of Electronic Materials 44, 1688–1696.

Xiang, X.D., Sun, X.D., Briceno, G., et al., 1995. A combinatorial approach to materials discovery. Science 268, 1738–1740.

Yamada, N., 1996. Erasable phase-change optical materials. MRS Bulletin 21, 48–50.

Yamamoto, A., Obara, H., Ueno, K., 2007. Optimization of thermoelectric properties of Ni-Cu based alloy through combinatorial approach. In: Hogan, T.P., Yang, J., Funahashi, R., Tritt, T. (Eds.), MRS Fall Meeting. Boston: Materials Research Society.

Yoo, Y.K., Tsui, F., 2002. Continuous phase diagramming of epitaxial films. MRS Bulletin 27, 316–323.

Yoo, Y.K., Ohnishi, T., Wang, G., et al., 2001. Continuous mapping of structure-property relations in $Fe_{1-x}Ni_x$ metallic alloys fabricated by combinatorial synthesis. Intermetallics 9, 541–545.

Yoo, Y.K., Xue, Q.Z., Chu, Y.S., et al., 2006. Identification of amorphous phases in the Fe-Ni-Co ternary alloy system using continuous phase diagram material chips. Intermetallics 14, 241–247.

Yu, M.H., Hattrick-Simpers, J., Takeuchi, I., et al., 2005. Interphase exchange coupling in Fe/Sm-Co bilayers with gradientFe thickness. Journal of Applied Physics 98, 063908.

Zarnetta, R., Takahashi, R., Young, M.L., et al., 2010. Identification of quaternary shape memory alloys with near-zero thermal hysteresis and unprecedented functional stability. Advanced Functional Materials 20, 1917–1923.

Zhang, K., Dice, B., Liu, Y., et al., 2015. On the origin of multi-component bulk metallic glasses: Atomic size mismatches and de-mixing. The Journal of Chemical Physics 143. 054501.

Zhao, J.C., 2006. Combinatorial approaches as effective tools in the study of phase diagrams and composition-structure-property relationships. Progress in Materials Science 51, 557–631.

Zheng, X., Cahill, D.G., Krasnochtchekov, P., Averback, R.S., Zhao, J.C., 2007. High-throughput thermal conductivity measurements of nickel solid solutions and the applicability of the Wiedemann-Franz law. Acta Materialia 55, 5177–5185.

Zhong, L., Wang, J., Sheng, H., Zhang, Z., Mao, S.X., 2014. Formation of monatomic metallic glasses through ultrafast liquid quenching. Nature 512, 177–180.